Chinese Chemical Letters 31 (2020) 2843–2848

Contents lists available at ScienceDirect

Chinese Chemical Letters

journal homepage: www.elsevier.com/locate/cclet

Communication

Effect of graphitic carbon nitride powders on adsorption removal of antibiotic resistance genes from water

Haiyin Zhan[a,1], Yutong Wang[a,1], Xueyue Mi[a], Zhiruo Zhou[a], Pengfei Wang[b,*], Qixing Zhou[a,*]

[a] College of Environmental Science and Engineering, Nankai University, Tianjin 300071, China
[b] School of Energy and Environmental Engineering, Hebei University of Technology, Tianjin 300401, China

ARTICLE INFO

Article history:
Received 15 June 2020
Received in revised form 7 August 2020
Accepted 11 August 2020
Available online 13 August 2020

Keywords:
Antibiotic resistance genes
Adsorption
Removal
Drinking water
g-C_3N_4

ABSTRACT

There is a growing need to eliminate antibiotic resistance genes (ARGs) in the environment and mitigate widespread antibiotic resistance. Graphitic carbon nitride (g-C_3N_4) was successfully synthesized *via* facile thermal polymerization approach and its potential for adsorption treatment of ARGs in water was examined. Batch adsorption experimental results revealed that g-C_3N_4 powders had robust adsorption activity for the gene *ampC* and *ermB*. Adsorption kinetics and isotherms were systematically investigated to explain the adsorption mechanism. The apparent adsorption equilibrium could be reached within 180 min. The adsorption process effectively removed ARGs (*ampC* and *ermB*) from water with 3.2 log and 4.2 log reductions, respectively. In addition, experimental data were analyzed by several models and simulated well with Langmuir isotherm and *pseudo*-second-order model. It indicated that adsorption process might be dominated by the chemical rate-limiting step. Moreover, the effects of temperature and pH on the removal of ARGs were conducted and the isoelectric point (IEP) was obtained. Finally, we have demonstrated that the g-C_3N_4 is a novel adsorbent and can be used as column packing to remove ARGs by filtration.

Antibiotics are widely used and often misused in human medicine and stockbreeding operations [1], which have led to the emergence and proliferation of antibiotic resistance genes (ARGs) in the environment [2]. What is worse is that ARGs could permanently exist even in the absence of antibiotic selective pressure [3]. ARGs also have the potential to be widely distributed to various environmental compartments [4,5]. To date, diverse kinds of ARGs have been detected in surface water [6], groundwater [7] and even in drinking water [8]. Aquatic ecosystems are recognized as reservoirs for ARGs and vehicle of antibiotic resistance. ARGs in water may pose the ubiquitous propagation of antibiotic resistance [9] and serious risks to both human health and ecosystem [10]. As one of the most critical human health challenges, ARGs have gained increasing attention all around the world [11]. Therefore, it is necessary to remove ARGs from the water environment (Text S1 in Supporting information).

Two kinds of ARGs are present in water, namely intracellular ARGs (iARGs) and extracellular ARGs (eARGs) [12]. iARGs are harbored *via* antibiotic resistance bacteria (ARB), and eARGs originate from the secretion of live ARB [13]. After entering the environment, eARGs are ready to be assimilated by indigenous competent bacteria *via* transformation [14]. When the bacteria harboring iARGs die, iARGs can be released to the environment again by the lysis of dead cells [15,16] and still stay bioavailable [17]. eARGs in the environment are relatively stable and often persisting for months [18]. The circulation of eARGs contributes to the widespread of antibiotic resistance, which emphasizes the demand for elimination of eARGs. However, a very limited number of attempts have been made to solve this problem. McKinney and Pruden [11] demonstrated that ultraviolet disinfection held weak potential to damage ARGs in water. Yuan *et al.* [19] demonstrated that the reductions of erythromycin and tetracycline resistance genes by chlorination were approximate 0.42 log and 0.10 log. Guo *et al.* [20] discovered that low dose of chlorine (40 mg Cl min/L) even promote horizontal

* Corresponding authors.
E-mail addresses: pengfeiwang@hebut.edu.cn (P. Wang), zhouqx@nankai.edu.cn (Q. Zhou).
[1] These authors contributed equally to this work and should be considered co-first authors.

https://doi.org/10.1016/j.cclet.2020.08.015
1001-8417/

gene transfer and spread of antibiotic resistance. Hence, the aforementioned methodologies have some limitations and it is urgent to explore more effective removal methods.

Adsorption technique has been extensively applied in wastewater treatment due to its ease of operation, high efficiency and economical cost [21]. The choice of adsorbent is an essential step for adsorption process. Graphitic carbon nitride (g-C_3N_4) with chemical stability and nontoxic property has captured the concern of numerous researchers [22]. Compared with common carbon materials (graphene, activated carbon, *etc.*), g-C_3N_4 has the advantages of high stability, low synthesis cost, high selectivity, easy regeneration and high recyclability, which well overcomes the typical defects of common environmental protection materials, such as poor selectivity and high energy consumption regeneration [23,24]. Meanwhile, due to its large specific surface area and abundant functional groups containing nitrogen on the surface, it can provide suitable sites for the adsorption of ARGs [25]. g-C_3N_4 an be easily synthesized from abundant precursors *via* the polymerization method [26], which is suitable for large scale production. Melamine [27], cyanamide [28], dicyandiamide [29], thiourea [30] and urea [31] are commonly used as precursors. As a nitrogen-rich and oxygen-containing compound, urea is low-cost and readily available. Nowadays, g-C_3N_4 has played important roles in degradation of organic pollutants [32], adsorption of heavy metal ions [33], photocatalytic reduction of CO2 [34] and NO [35]. However, to the best of our knowledge, the adsorption of ARGs on g-C_3N_4 has never been reported. In this study, our attention is focused on two representative eARGs (*ampC* and *ermB*). β-Lactam antibiotics are the most consumed antibiotics globally [36], and the gene *ampC* encoding resistance to β-lactam has been detected in wastewater, surface water, and even from drinking water films [37]. Meanwhile, the gene *ermB* (against macrolides) is one of the most prevalent erythromycin resistance genes in the environment [38].

The objective of this study is to examine the potential of g-C_3N_4 for removing eARGs from water. We employed the thermal polymerization method to synthesize g-C_3N_4 powders with urea as a precursor. A series of adsorption experiments were performed with the as-prepared g-C_3N_4. Quantitative real-time polymerase chain reaction (qPCR) was used to determine the concentrations of the target ARGs in aqueous solution. g-C_3N_4 powders were systematically characterized by scanning electron microscope (SEM), transmission electron microscope (TEM), X-ray diffraction (XRD), Brunauer-Emmett-Teller (BET) surface area, Fourier transform infrared (FTIR), X-ray photoelectron spectroscopy (XPS). The zeta potentials of the g-C_3N_4 powders and ARGs were measured and the isoelectric point (IEP) was discussed. Adsorption isotherms and kinetics were investigated to confirm the adsorption capacity of g-C_3N_4. We also took into consideration of two parameters (pH and temperature) in the experiment. The mechanisms that underline the adsorption process were explored and analyzed. Furthermore, we fabricated a column to remove ARGs by filtration and validated its efficiency.

Detailed information on the synthesis, characterization, sample collection, ARGs extraction and adsorption experiments of g-C_3N_4 is provided in the Texts S2-5 (Supporting information). SEM, TEM, XPS, XRD, FTIR, nitrogen adsorption-desorption isotherm and pore diameter distribution analysis were shown in Text S6 (Supporting information).

Adsorption is a physicochemical process that involves mass transfer of solute from liquid phase to the surface of adsorbent [39]. Kinetics study can provide necessary information to describe the adsorption rate of g-C_3N_4 and control the residual time of the whole adsorption process [40]. The adsorption kinetics were investigated by adding the as-prepared g-C_3N_4 powders to the solutions containing the target ARGs. Initial concentrations of *ampC* and *ermB* were examined and recorded. The time-dependent adsorption curves of *ampC* and *ermB* are depicted in Fig. 1a. It is apparent that with the passage of time, the values of $\lg C_0/C$ for both ARGs continually increase. This experiment maintains a continuous and homogeneous adsorption process. There are no significant differences in the trends of two curves. The adsorption equilibrium for both ARGs can be achieved within 180 min. The $\lg C_0/C$ values of two ARGs (*ampC* and *ermB*) at equilibrium are 3.2 and 4.2, indicating good efficiency of g-C_3N_4 as an adsorbent. Actually, the adsorption rate of *ermB* on g-C_3N_4 is higher than that of *ampC*, reflected by the higher initial slope of the adsorption kinetic curve, which can be attributed to the deoxyribonucleic acid (DNA) length

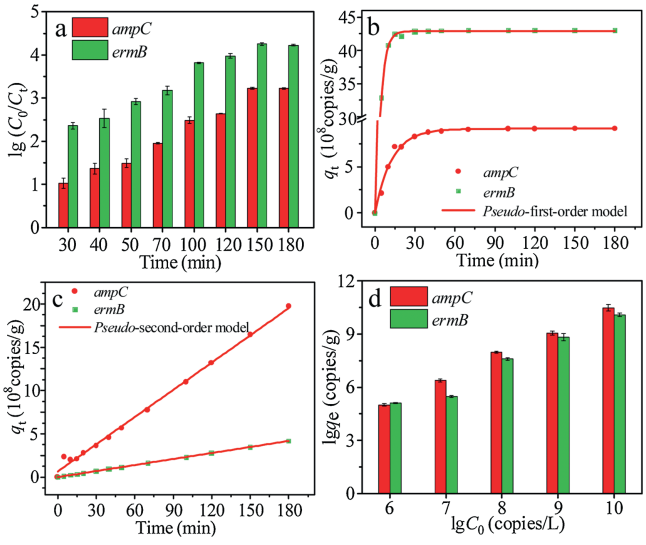

Fig. 1. Adsorption kinetics of ARGs on g-C_3N_4 powders (a). The fitting curves of adsorption kinetics: *Pseudo*-first-order model (b), and *pseudo*-second-order model (c). The adsorption capacity ($\lg q_e$) changes with initial ion concentration ($\lg C_0$) at room temperature (d).

of *ermB* (189 bp) is shorter than that of *ampC* (193 bp). In a study by Wu *et al.* [41], shorter DNA are adsorbed more rapidly and bind more tightly to the surface of graphene oxide. Li and Rothberg [42] have demonstrated that the adsorption rate of single-stranded DNA depend on DNA length and temperature. Subsequently, they have further confirmed that longer single-stranded DNA sequences were adsorbed on the Au nanoparticles at a much slower rate [43]. In this study, the results are in accordance with previous researches. In addition, the adsorption of ARGs on g-C_3N_4 may be related to its base composition [44,45].

For the sake of evaluating the adsorption mechanism in depth, the *pseudo*-first-order and *pseudo*-second-order models were used to analyze the data of adsorption kinetics. The two models can be described by equations (Eqs. 1 and 2), respectively.

$$q_t = q_e \times (1 - e^{-k_1 \cdot t}) \tag{1}$$

$$\frac{t}{q_t} = \frac{t}{q_e} \times \frac{1}{q_e^2 \times k_2} \tag{2}$$

where q_t (copies/L) and q_e (copies/g) are the amounts of ARGs adsorbed on the g-C_3N_4 at time t (min) and at equilibrium, respectively. k_1 (min^{-1}), k_2 (copies $g^{-1}\,min^{-1}$) are the rate constants of two models. The k_1, k_2 and q_e could be calculated from the slope and intercept of the curves.

The correlation coefficient R^2 is important to estimate the suitability of different equation models. The higher the value of R^2 is, the more accurately the model describes the adsorption kinetics. The results are summarized in Table S2 (Supporting information). As shown in Figs. 1b and c, the *pseudo*-second-order model provided better fitting for all the experimental data. The correlation coefficients are higher than 0.994, indicating that in this experiment adsorption is probably dominated by a monolayer adsorption [46]. The adsorption of g-C_3N_4 to ARGs may be due to the triazine ring fabricating by C and N atoms which form the highly delocalized π conjugated system through sp^2 hybridization, providing a possibility to fix the DNA molecule on it by π-π bond adsorption because of the π conjugated on the nucleotide [47]. In addition, the nitrogen of base ring and the exocyclic keto groups of ARGs may also be responsible for the binding of ARGs to g-C_3N_4 through chemical binding on amine groups and other surface groups on g-C_3N_4. The rate-limiting step may involve valency forces through sharing or the exchange of electrons [48]. The q_e of *ermB* was larger than that of *ampC*. Their values of k_2 were also in the order of *ermB* > *ampC*. It indicated that the length of DNA may affect the adsorption process.

To determine the maximum adsorption capacity, the experiments of adsorption isotherms were carried out with varied initial concentrations of ARGs at room temperature. Preliminarily tests indicated experimental time was supposed to be set longer than 180 min. As shown in Fig. 1d higher C_0 values brought in higher values of q_e. The adsorption capability increased with the rise of initial concentrations for both the gene *ampC* and *ermB*. Driving force generated by the pressure of concentration gradient could account for these phenomena. The interaction between the adsorbate and adsorbent can be described by two common isotherm equilibrium models, namely the Langmuir and Freundlich models. The equations of the two models can be expressed as follows (Eqs. 3 and 4):

$$\frac{1}{q_e} = \frac{q}{q_m} + \frac{1}{b \times q_m} \times \frac{1}{C_e} \tag{3}$$

$$\log q_e = \log k_f + \frac{1}{n} \times \log C_e \tag{4}$$

In these equations, q_m (copies/g) is the maximum adsorption amount; C_e (copies/L) is the equilibrium concentration; b, k_f and n are the constants of two models.

The parameters of the two models were listed in Table S3 (Supporting information). The linear fitting results of Langmuir model and Freundlich model are shown in Fig. 2. The maximum adsorption capacities of *ampC* and *ermB* at 25 °C are 7.2×10^5 copies/g and 10.6×10^5 copies/g, separately. The correlation coefficients (R^2) of Langmuir model for *ampC* and *ermB* are both above 0.97, higher than those of Freundlich model (0.60 for *ampC* and 0.93 for *ermB*). The experimental data are better simulated by the Langmuir model. In fact, the Langmuir isotherm is generally established on the assumption that the surface of the absorbent is homogenous, which means every adsorption site has equal affinity with the adsorbate. In this experiment, it means a monolayer adsorption, which is suitable for the adsorption of *ampC* and *ermB* on g-C_3N_4 powders. In addition, R_L, namely the separation factor, is an essential characteristic of the Langmuir isotherm to predict the affinity, which could be calculated from the following equation (Eq. 5) [49].

$$R_L = \frac{1}{1 + bC_0} \tag{5}$$

If the value of R_L is within the range of 0–1, the process is favorable [50]. In these works, all of the R_L values were between 0 and 1 which indicated that g-C_3N_4 was a favorable adsorbent for the removal of ARGs (Table S4 in Supporting information).

We also investigated the influence of different experimental temperatures on the adsorption process. We placed the experimental facility in the working conditions where the temperature has already been set. As shown in Fig. 3a, the reductions of two genes (*ampC* and *ermB*) are 3.4–3.6 log and 4.1–4.4 log,

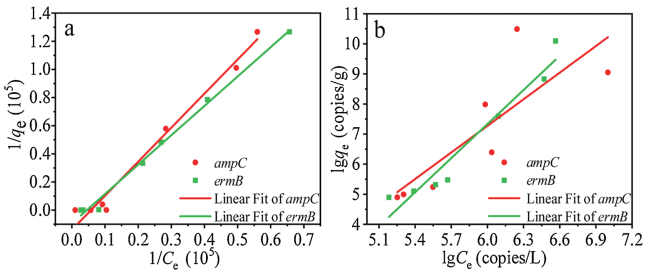

Fig. 2. The linear fits of Langmuir model (a) and Freundlich model (b).

respectively. There were no significant differences in the values of each gene among the three temperatures in Figs. 3a and b ($P > 0.05$). It is obvious that experimental temperature has no effect on the removal of ARGs. This conclusion is in accordance with the findings of Wang and his colleagues [13]. These results also indicate that g-C_3N_4 powders maintain stable adsorption capability in a wide temperature range of 4−40 °C.

The pH of the solution is also an important factor in the absorption process. The adsorption efficiency of ARGs on the g-C_3N_4 at the wide pH values ranging from 2.0 to 11.0 is shown in Fig. 4a. Duplicate samples were done for each pH data point. The removals of two ARGs were both significantly affected by the pH of the solution. In this study, acidic or neutral conditions (pH from 2.0 to 7.0) were more beneficial than alkaline condition (pH at 8.0–11.0) for the absorption process. As the pH values increases, the lgC_0/C value drops gradually. Obvious reductions of gene copy number with above 4.0 log for *ermB* and 2.9 log for *ampC* are observed ($2.1 < pH < 5.6$). They can also reach over 3.0 log for *ermB* and 2.0 log for *ampC* when the pH values are in the range of 5.6−8.8. However, the absorption amounts for both ARGs were obviously reduced at $pH > 8.8$. It could be seen that the pH of the solution has an obvious effect on the adsorption process. The binding strength between DNA and adsorbent can be conveniently controlled by tuning the solution pH [41]. Li *et al.* [51] has revealed that DNA strongly bound to multilayer amine modified surfaces under pH 5.6 buffer, when the majority of surface amine groups were protonated. Our investigation results are in agreement with these researches, showing that absorption capacities can be influenced by pH.

According to previous studies, g-C_3N_4 and eARGs are both ampholytes with pivotal physicochemical properties. IEP is an essential parameter which is able to characterize the adsorption properties of materials. The surface charge of ampholytes is positive when the pH value of the environment is below its IEP. In contrast, it is negative above its IEP [52]. The zeta potentials were measured to further investigate the surface charge of the g-C_3N_4 powders in aqueous suspensions and understand the adsorption mechanisms. Triplicate samples were done for each pH effect data point and the average values were presented in Fig. 4b. In the suspension with the initial pH, the zeta potential of g-C_3N_4 is 39.2 mV. As the pH of aqueous suspensions increases, zeta potentials decrease continuously. The IEP of g-C_3N_4 is approximate 5.0. At $pH < 5.0$, the surface charge of the g-C_3N_4 is positive owing to the protonation reaction, whereas deprotonation reaction occurs and the surface of g-C_3N_4 turns negative at $pH > 5.0$. The protonation-deprotonation transition of g-C_3N_4 in aqueous suspensions involves interactions among hydrogen ions, hydroxyl ions, and certain groups on the g-C_3N_4 surface. The zeta potential curves obtained for the two ARGs exhibited similar tendency. The zeta potentials of *ampC* steadily decrease from 7.45 mV (in strong acidic conditions) to −42.4 mV (in strong basic conditions). On the basis of above analysis, the IEP of *ampC* is about 3.0 and the IEP of *ermB* is 3.2 or so. When the pH value is above 5.0, the adsorbates and adsorbent are both negatively charged with similar potentials. Electrostatic interaction makes strengthen action in the adsorption process. ARGs should be repelled by the g-C_3N_4 due to intense electrostatic repulsion. Therefore, the adsorption effect is not ideal.

We have verified that the g-C_3N_4 powders can be served as column packing. Removal of pollutants in water by an adsorption column is an attractive technique, because it allows non-stop operation [53]. We fabricated a short column to purify water by filtration. A syringe (the volume capacity is 12 mL and the diameter is 1.8 cm) was chosen as the column, and g-C_3N_4 powders were added into the column. A slice was placed at the bottom to prevent the powders from leaking from the syringe. During the filtration process, the concentration of the effluent and corresponding time were recorded. As shown in Fig. 5a, at the beginning, the concentration of outflow is relatively close to the initial concentration, indicating the adsorption efficiency of the column is unremarkable. The reason for this phenomenon is that the adsorbents (compact g-C_3N_4 powders) have loose contact with the target ARGs in solutions. The adsorption rate could be limited by the diffusion of adsorbate molecules through the column. The values of lgC_0/C gradually increase with the permeation volume. 50 mL solution was fully filtered through the column. The final reductions of ARGs were 1.7 log for *ampC* and 3.0 log for *ermB*. As time went on, the adsorption amounts of g-C_3N_4 powders steadily rose (Fig. 5b). The filtration process was completed in 22 min and the average adsorption rate was 2.3 mL/min. In fact, the total adsorption amounts of g-C_3N_4 powders by a column were lowerthan those by directly adding g-C_3N_4 powders to solution. It mainly depended on diffusion and contact between the adsorbent and the adsorbate. The more fully g-C_3N_4 powders contact with ARGs, the better results the process achieve. The contact time was determined by the flow rate, which could affect the adsorption capacity to a great degree and the effect of flow rate remains further study.

In conclusion, an adsorption process using g-C_3N_4 powders as a novel adsorbent was employed to removal eARGs from water. The g-C_3N_4 powders were successfully prepared in a facile method and convenient for large-scale production. The concentration of two representative ARGs were measured with qPCR technique. ARGs (*ampC* and *ermB*) were effectively removed in the adsorption process with a 3.2 log and 4.2 log reductions, compared with other treatment technologies and other adsorption materials, it has good adsorption performance (Text S7 in Supporting information). Langmuir isotherm and *pseudo*-second-order model were proven to be well fitted with the experimental data. The pH value of the solution could affect the adsorption capacity of g-C_3N_4 powders. In terms of the absorption process, acidic or neutral conditions (pH from 2.0 to 7.0) were more beneficial than alkaline condition. Furthermore, the adsorbent maintains good adsorption capability

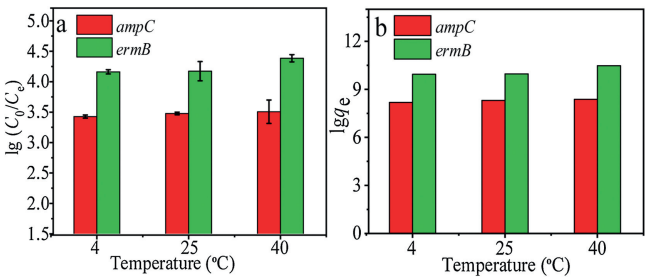

Fig. 3. Effect of different temperatures on the adsorption capacity (a and b).

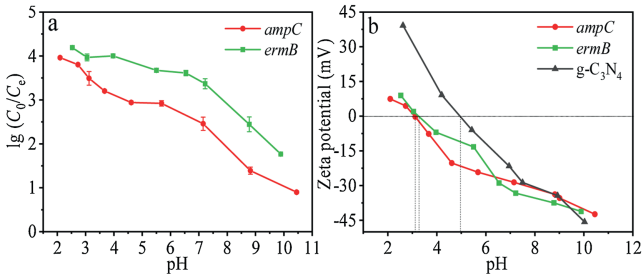

Fig. 4. Effect of various pH values on the adsorption capacity of g-C_3N_4 powders (a), and the zeta potentials of g-C_3N_4 and two ARGs in aqueous suspensions (b).

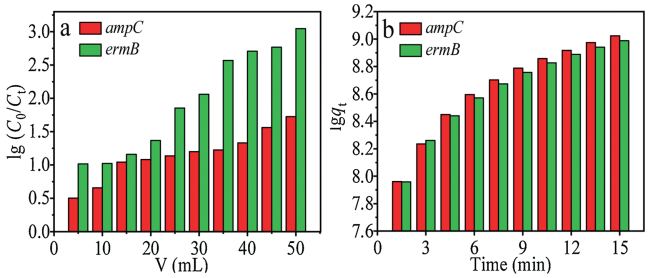

Fig. 5. The differences between the concentration of inflow and outflow as a function of permeation volume (a), and adsorption amounts of the column *versus* time (b).

in a wide temperature range of 4–40 °C and can be served as column packing to purify water by filtration. Based on bulk availability and superior removal performance, g-C_3N_4 is a promising candidate for the effective adsorption of ARGs from water.

Declaration of competing interest

The authors report no declarations of interest.

Acknowledgments

The authors gratefully acknowledge the financially support by the National Natural Science Foundation of China as general projects (Nos. 21677080 and 21722702), and the Natural Science Foundation of Hebei Province (No. B2019202078).

Appendix A. Supplementary data

Supplementary material related to this article can be found, in the online version, at doi:https://doi.org/10.1016/j.cclet.2020.08.015.

References

[1] S.P. Rong, Y.B. Sun, Z.H. Zhao, Chin. Chem. Lett. 25 (2014) 187–192.
[2] J. Davies, D. Davies, Microbiol. Mol. Biol. Rev. 74 (2010) 417–433.
[3] D.I. Andersson, D. Hughes, FEMS Microbiol. Rev. 35 (2011) 901–911.
[4] Y. Agersø, D. Sandvang, Appl. Environ. Microb. 71 (2005) 7941–7947.
[5] C. Rodriguez, L. Lang, A. Wang, K. Altendorf, et al., Appl. Environ. Microb. 72 (2006) 5870–5876.
[6] F.F. Reinthaler, J. Posch, G. Feierl, et al., Water Res. 37 (2003) 1685–1690.
[7] J.C. Chee-Sanford, R.I. Aminov, I.J. Krapac, et al., Appl. Environ. Microb. 67 (2001) 1494–1502.
[8] C.W. Xi, Y.L. Zhang, C.F. Marrs, et al., Appl. Environ. Microb. 75 (2009) 5714–5718.
[9] J. Li, B. Shao, J.Z. Shen, et al., Environ. Sci. Technol. 47 (2013) 2892–2897.
[10] A. Pruden, R. Pei, H. Storteboom, K.H. Carlson, Environ. Sci. Technol. 40 (2006) 7445–7450.
[11] C.W. McKinney, A. Pruden, Environ. Sci. Technol. 46 (2012) 13393–13400.
[12] K.M. Nielsen, P.J. Johnsen, D. Bensasson, D. Daffonchio, Environ. Biosaf. Res. 6 (2007) 37–53.
[13] D.N. Wang, L. Liu, Z.G. Qiu, et al., Water Res. 92 (2016) 188–198.
[14] D.Q. Mao, Y. Luo, J. Mathieu, et al., Environ. Sci. Technol. 48 (2014) 71–78.
[15] G. Pietramellara, J. Ascher, F. Borgogni, et al., Biol. Fertil. Soils 45 (2009) 219–235.
[16] D.J. Levy-Booth, R.G. Campbell, R.H. Gulden, et al., Soil Biol. Biochem. 39 (2007) 2977–2991.
[17] N.X. Lu, J.L. Zilles, T.H. Nguyen, Appl. Environ. Microb. 76 (2010) 4179–4184.
[18] B. Zhu, Water Res. 40 (2006) 3231–3238.
[19] Q.B. Yuan, M.T. Guo, J. Yang, PLoS One 10 (2015) e0119403.
[20] M.T. Guo, Q.B. Yuan, J. Yang, Environ. Sci. Technol. 49 (2015) 5771–5778.
[21] W.W. He, N. Li, X. Wang, T.L. Hu, X.H. Bu, Chin. Chem. Lett. 29 (2018) 857–860.
[22] G.C. Sun, F.Z. Zhang, Q.S. Xie, W. Luo, J.P. Yang, Chin. Chem. Lett. 31 (2020) 1603–1607.
[23] Y.H. Wu, Q. Chen, S. Liu, et al., Chin. Chem. Lett. 30 (2019) 2186–2190.
[24] Y.Y. Zhang, Z.X. Zhou, Y.F. Shen, ACS Nano 10 (2016) 9036–9043.
[25] R. Hu, X.K. Wang, S.Y. Dai, et al., Chem. Eng. J. 260 (2015) 469–477.
[26] M. Groenewolt, M. Antonietti, Adv. Mater. 17 (2005) 1789–1792.
[27] H.S. Zhai, L. Cao, X.H. Xia, Chin. Chem. Lett. 24 (2013) 103–106.
[28] S. Hwang, S. Lee, J.S. Yu, Appl. Surf. Sci. 253 (2007) 5656–5659.
[29] D.Y. Ni, Y.Y. Zhang, Y.F. Shen, S.Q. Liu, Y.J. Zhang, Chin. Chem. Lett. 31 (2020) 115–118.
[30] M.X. Ran, P. Chen, J.R. Li, et al., Chin. Chem. Lett. 30 (2019) 875–880.
[31] F. Dong, L.W. Wu, Y.J. Sun, et al., J. Mater. Chem. 21 (2011) 15171–15174.
[32] M. Ding, J.J. Zhou, H.C. Yang, et al., Chin. Chem. Lett. 31 (2020) 71–76.
[33] Q. Liu, D.B. Zhu, M.L. Guo, Y. Yu, Y.J. Cao, Chin. Chem. Lett. 30 (2019) 1639–1642.
[34] Y.P. Chen, H.Y. Zhang, R. Lu, A.C. Yu, Chin. Chem. Lett. 29 (2018) 543–546.
[35] F. Dong, Z.Y. Wang, Y.H. Li, et al., Environ. Sci. Technol. 48 (2014) 10345–10353.
[36] Q.K. Chen, L. Chen, J.J. Qi, et al., Chin. Chem. Lett. 30 (2019) 1214–1218.
[37] T. Schwartz, W. Kohnen, B. Jansen, U. Obst, FFEMS Microbiol. Ecol. 43 (2003) 325–335.
[38] A. Di Cesare, D. Fontaneto, J. Doppelbauer, G. Corno, Environ. Sci. Technol. 50 (2016) 10153–10161.
[39] Y. Li, M.Q. Li, J. Zhang, X.Y. Xu, Chin. Chem. Lett. 30 (2019) 762–766.
[40] L. Fan, C. Luo, X. Li, et al., J. Hazard. Mater. 215–216 (2012) 272–279.
[41] M. Wu, R. Kempaiah, P.J. Huang, et al., Langmuir 27 (2011) 2731–2738.
[42] H.X. Li, L.J. Rothberg, J. Am. Chem. Soc. 126 (2004) 10958–10961.
[43] H.X. Li, L.J. Rothberg, Anal. Chem. 76 (2004) 5414–5417.

[44] S.J. Sowerby, C.A. Cohn, W.M. Heckl, N.G. Holm, Proc. Natl. Acad. Sci. U. S. A. 98 (2001) 820–822.
[45] S. Gowtham, R.H. Scheicher, R. Ahuja, R. Pandey, S. Karna, Phys. Rev. B 76 (2007) 033401.
[46] X.Y. Sun, P.Z. Zhang, B. Ai, Y.B. Wang, Chin. Chem. Lett. 27 (2016) 139–144.
[47] M.J. Chang, W.N. Cui, J. Liu, K. Wang, X.J. Chai, J. Mater. Sci. Mater. Electron. 29 (2018) 6771–6778.
[48] Y.S. Ho, G. McKay, Water Res. 34 (2000) 735–742.
[49] M.S. Chiou, P.Y. Ho, H.Y. Li, Dyes Pigm. 60 (2004) 69–84.
[50] M. Wu, R. Kempaiah, P.J. Huang, V. Maheshwari, J. Liu, Langmuir 27 (2011) 2731–2738.
[51] Z. Li, K.M. Ashraf, M.M. Collinson, D.A. Higgins, Langmuir 33 (2017) 8651–8662.
[52] M. Wang, Y.X. Liu, D. Li, J.W. Tang, W.X. Huang, Chin. Chem. Lett. 30 (2019) 985–988.
[53] Y.Q. Chen, L.B. Chen, H. Bai, L. Lei, J. Mater. Chem. A 1 (2013) 1992–2001.